# Example Applications of A Stochastic Ground Motion Simulation Methodology in Structural Engineering

**S. Rezaeian & N. Luco**
*U.S. Geological Survey, Golden, CO, USA*

**ABSTRACT:**
Example engineering applications of a stochastic ground motion simulation methodology are presented. This simulation methodology, which was recently developed by the first author, is used to generate synthetic accelerograms for specified design scenarios. Each design scenario is defined by earthquake and site characteristics such as the faulting mechanism, earthquake magnitude, source-to-site distance, and soil conditions. The simulation model is developed to realistically represent characteristics of real earthquake ground motions such as the time-varying intensity and frequency content of the motion. These characteristics can greatly influence the structural response. Furthermore, the natural variability of recorded motions is captured in the simulations, which facilitates quantification of the variability in the structural response due to variations in the input excitation. In this paper, example structural analyses are provided and the resulting structural responses and their statistics are scrutinized. We consider three types of seismic performance assessments that are described in the new ATC-58 guidelines. First, we demonstrate how ground motion simulations can be used to perform *intensity-based assessments*, where the intensity of ground motion is specified in addition to the design scenario. Then, accounting for the uncertainty in the shaking intensity, we perform *scenario-based assessments*, where only the design scenario is specified. Finally, we describe how our method can be extended to perform *time-based assessments*, where all possible design scenarios and their probability of occurrences are considered.

*Keywords: Stochastic Ground Motion Simulation, Engineering Applications, Structural Response*

## 1. INTRODUCTION

Many ground motion simulation models have been developed in the past few decades, but their use in engineering practice has been limited in most regions of the United States. Despite the fact that current building codes permit the use of appropriate simulated ground motions, engineers typically refrain from doing so due to reasons such as model complexities, lack of understanding the underlying seismological principles, limited knowledge of the model parameters, or simply lack of guidelines on applications of these models.

On the other hand, the scarcity of recorded earthquake ground motions necessitates simulation of ground motions, particularly with the advent of performance-based earthquake engineering (PBEE). PBEE attempts to consider the entire range of seismic hazards and structural behaviors to minimize the overall risk and life-cycle cost. This range includes nonlinear behavior and even collapse of structures. Therefore, in PBEE, an ensemble of ground motions that represents all possible realizations for specified design scenarios (i.e., earthquake of given characteristics at a given site) is of interest. In the current engineering practice, input excitations for response history dynamic analysis are selected from a database of ground motions recorded during past earthquakes. For many design scenarios of interest, recorded motions are sparse or lacking. As a result, engineers are often forced to significantly alter recorded motions by various scaling and frequency matching methods in order to achieve the desired intensity or frequency characteristics of a target design response spectrum that is constructed for a specified design scenario. These modifications have raised concern about the validity of the approach, as the modified motions may not accurately represent real earthquake ground motions. In the past decade, there have been major advancements in PBEE, but the scarcity of appropriate input ground motions for response history analysis remains one of the major shortcomings of this approach. This paper helps advance the practice of PBEE by presenting example structural analyses that use ground motion simulations as input excitations. This can be useful when recorded motions are scarce or nonexistent for design scenarios of interest.

In our examples, we consider three types of seismic performance assessments that are similar to those described in the Next-Generation Performance-Based Seismic Design Guidelines by the Applied Technology Council (ATC-58-1, 2011). The three types of performance assessments are: intensity-based, scenario-based, and time-based.

Intensity-based assessment evaluates a building's probable performance assuming that it is subjected to a specific intensity of shaking. Shaking intensity, in the form of 5% damped elastic acceleration response spectrum, is specified in addition to the design scenario (i.e., earthquake and site characteristics) in order to efficiently estimate the structural responses with few ground motions. This approach is commonly taken by practicing engineers as it is convenient and is specified in current building codes (per ASCE7 guidelines). In this paper, we present a procedure that generates a suite of simulated ground motions for a given design scenario and a specified intensity of shaking. Example structural analyses, the resulting structural responses, and their statistics are presented.

Scenario-based assessment evaluates a building's probable performance assuming that it is subjected to the effects of a specific design scenario. A design scenario is defined by the earthquake and site characteristics, which in this paper are the faulting mechanism, earthquake magnitude, source-to-site distance, and soil conditions. These factors are the input parameters to our ground motion simulation model. Scenario-based assessment considers all shaking intensities that can be caused by the specified design scenario. In this way, the variability in the intensity of shaking is accounted for. We demonstrate how this approach can be used to predict the probability distribution of the structural response and determine failure probabilities for a specified design scenario. The next generations of seismic design procedures are moving towards scenario-based assessments.

Finally, time-based assessment evaluates a building's performance over a period of time, considering all possible design scenarios and their probability of occurrences in that period of time. This type of seismic assessment considers uncertainty in the design scenario as well as in the shaking intensity. We discuss how our simulation method can be used to extend a scenario-based assessment to a time-based assessment.

We begin this paper by summarizing the stochastic ground motion simulation methodology used in this study. Then the details of our structural analyses including the buildings under consideration, the earthquake design scenarios, the simulated input ground motions, and the structural analysis technique are presented. The results of structural analyses are discussed next. Structural responses for specified shaking intensities and design scenarios (i.e., intensity-based assessment) are given and their statistics are compared to those of similar studies in the literature. Next, structural responses for specified design scenarios (i.e., scenario-based assessment) and their applications in probabilistic studies are presented. Finally, extension of our methods to perform time-based assessment is discussed.

## 2. STOCHASTIC GROUND MOTION MODEL

In this study we use the stochastic ground motion model developed by Rezaeian and Der Kiureghian (2010). This model represents acceleration time-series as the response of a linear filter with time-varying parameters to white-noise excitation. The filter response is normalized by its standard deviation and is multiplied by a deterministic time-modulating function. While modulation of the process in time introduces temporal nonstationarity (variation of the intensity in time), time-variation of the filter parameters provides spectral nonstationarity (variation of the frequency content in time). Normalization by the standard deviation of the process prior to time-modulation separates the spectral and temporal nonstationary characteristics of the process, thus greatly facilitating modeling and parameter identification. In the continuous form, the model is formulated as

$$x(t) = q(t, \boldsymbol{\alpha}) \left\{ \frac{1}{\sigma_h(t)} \int_{-\infty}^{t} h[t-\tau, \boldsymbol{\lambda}(\tau)] w(\tau) \mathrm{d}\tau \right\} \quad (2.1)$$

where $x(t)$ is the acceleration time-series; $q(t, \boldsymbol{\alpha})$ is a deterministic time-modulating function with parameters $\boldsymbol{\alpha}$ controlling its shape and intensity; $w(\tau)$ is a white-noise process; the integral inside the curved brackets is a filtered white-noise process, where $h[t-\tau, \boldsymbol{\lambda}(\tau)]$ denotes the impulse-response function (IRF) of the filter with time-varying parameters $\boldsymbol{\lambda}(\tau)$; and $\sigma_h^2(t) = \int_{-\infty}^{t} h^2[t-\tau, \boldsymbol{\lambda}(\tau)] d\tau$ is the variance of the integral process. Due to the normalization by $\sigma_h(t)$, $q(t, \boldsymbol{\alpha})$ equals the standard deviation of $x(t)$ and completely controls the temporal characteristics of the process. On the other hand, the form of the IRF and its time-varying parameters control the spectral characteristics of the process. The time-modulating function and the linear filter employed in this study are similar to those used in Rezaeian and Der Kiureghian (2010).

The modulating function has three parameters, $\boldsymbol{\alpha} = (I_a, D_{5-95}, t_{mid})$. These parameters respectively represent: Arias intensity of the acceleration process; the effective duration of the motion, defined as the time interval between 5% and 95% of Arias intensity; and the time at the middle of the strong-shaking phase of the motion, defined as the time at which the 45% level of Arias intensity is reached. The selected filter also has three parameters, $\boldsymbol{\lambda} = (\omega_{mid}, \omega', \zeta)$. Parameters $\omega_{mid}$ and $\omega'$ represent the frequency of the filter, assumed to change linearly with time. $\omega_{mid}$ is the filter frequency at time $t_{mid}$ and $\omega'$ is the rate of change of the frequency with time. $\zeta$ represents the damping ratio of the filter, assumed to be constant with time. These parameters control the predominant frequency and bandwidth of the ground motion process.

Predictive equations for the six model parameters, $(I_a, D_{5-95}, t_{mid}, \omega_{mid}, \omega', \zeta)$, are developed empirically by identifying these parameters for many recorded motions with known earthquake and site characteristics. The empirical equations have the generic form of

$$\Phi^{-1}[F_\theta(\theta)] = \mu(F, M, R_{rup}, V_{S30}; \boldsymbol{\beta}) + \eta + \sigma \quad (2.2)$$

where $\theta$ represents one of the six model parameters, $\Phi^{-1}[.]$ is the inverse of the standard normal cumulative distribution function and $F_\theta(.)$ is the cumulative distribution function of $\theta$. As a result, the left hand side of Eqn. 2.2 transforms a model parameter from the physical space to the standard normal space. $F_\theta(.)$ is determined empirically and is given for each $\theta$ in Rezaeian and Der Kiureghian (2010). $\mu$ represents the predicted mean, which is a function of the earthquake and site characteristics and the vector of regression coefficients $\boldsymbol{\beta}$. The earthquake and site characteristics are represented by four variables that are commonly available to a design engineer. $F$ represents the faulting mechanism and assumes values of 0 and 1 for strike-slip and reverse types of faulting, respectively. $M \geq 6.0$ is the moment magnitude; $10 \leq R_{rup} \leq 100$km is the closest distance from the site to the ruptured area; and $V_{S30} \geq 600$m/s represents the average shear-wave velocity in the top 30 meters of the site. The limits on these variables are imposed mainly due to the database of recorded ground motions that was used to develop our empirical equations. The lower limit of 10km on $R_{rup}$ is to exclude the effects of near-fault directivity pulses. A companion study by Dabaghi et al. (2011) presents a method for simulation of near-fault ground motions, which removes the 10km boundary on $R_{rup}$. Further studies can be conducted in the future to develop similar empirical models for softer soil conditions with $V_{S30} <$ 600m/s. Finally, in Eqn. 2.2, $\eta$ and $\sigma$ are zero-mean normally distributed random variables that respectively denote the inter-event error (error among data belonging to different earthquakes) and the intra-event error (error among the data belonging to records of an individual earthquake). The regression coefficients, the variances of the error terms, and the correlations between the model parameters are identified empirically and are presented in Rezaeian and Der Kiureghian (2010).

In summary, if a design scenario is defined by the four variables, $F, M, R_{rup}$, and $V_{S30}$, the empirical predictive equations of the form given in Eqn. 2.2 can be used to generate realizations of the stochastic model parameters. Each set of realizations can then be used in Eqn. 2.1 to generate simulated time-series. To facilitate digital simulation, a discretized form of Eqn. 2.1 can be used (see Rezaeian and Der Kiureghian, 2010). When realizations of $x(t)$ are generated, they must undergo a high-pass filtering process to assure zero residual velocity and displacement, as well as to avoid overestimation of response spectral ordinates at long periods. For the high-pass filter, we use a critically damped oscillator with a corner frequency of $\omega_c = 0.1$Hz. The corrected acceleration record, denoted $z''(t)$, is obtained as the solution of the differential equation

$$z''(t) + 2\omega_c z'(t) + \omega_c^2 z(t) = x(t) \tag{2.3}$$

In Rezaeian and Der Kiureghian (2010), the response spectra of simulated motions and their variability are validated by comparisons to recorded ground motions and by comparisons to some ground motion prediction equations (GMPEs) that are widely-used in practice. The simulation model under consideration is extended to generate synthetic orthogonal horizontal components of ground motion in Rezaeian and Der Kiureghian (2012). In this paper, however, we only simulate one horizontal component for simplicity in the structural analysis.

### 2.1. Advantages and constraints of the model

The stochastic ground motion model discussed above has a number of important advantages for our study. (1) It realistically represents the time-varying intensity and frequency content of earthquake ground motions. These characteristics control properties of the input excitation such as the peak intensities, duration of motion, and predominant frequency, which are known to greatly influence the structural response. (2) Modeling is done entirely in the time-domain, is simple and requires little more than generation of standard normal random variables. There is no need for complicated procedures to process a target accelerogram, such as the Fourier analysis or estimation of evolutionary power spectral density. Hence, it is computationally efficient and easy to implement by practicing engineers. (3) The model has a small number of input parameters that describe a design scenario and are readily available to a design engineer. Therefore, the model can be practically used as a black-box simulation tool that takes $F, M, R_{rup}$, and $V_{S30}$ as input parameters and generates realizations of possible ground motions for a specified design scenario. (4) The simulated ground motions have realistic response spectra unlike recorded ground motions that are scaled or spectrum-matched to represent a Uniform Hazard Spectrum and often result in motions with unrealistic energy contents. (5) Finally, because the simulation method accounts for the uncertainty in the model parameters (by randomizing the error term in Eqn. 2.2) as well as the stochasticity of the acceleration process (provided by the white-noise excitation in Eqn. 2.1), it captures the natural variability of real ground motions given a design scenario. Therefore, this model is adequate for performing probabilistic analyses and can be used to quantify the variation of the structural response due to the variation in input excitation.

The stochastic model given in Eqn. 2.1 is only valid for simulating ground motions without near-fault effects such as directivity pulses. Hence, the distance is restricted to a minimum of 10km. To simulate ground motions with directivity effects, one can simulate a velocity pulse which can be differentiated and added to Eqn. 2.1. Such a model is presented in Dabaghi et al. (2011), where empirical equations are developed for the parameters of the velocity pulse as functions of earthquake and site characteristics. In this paper, for simplicity, we do not consider near-fault directivity effects.

The empirical equations represented by Eqn. 2.2 are applicable for simulating free-field strong ground motions on firm soil that are generated from shallow crustal earthquakes in tectonically active regions. These restrictions are due to the limitations of the selected database of recorded ground motions used in empirical modeling. This database was a subset of the Next Generation Attenuation database (see

Campbell and Bozorgnia, 2008) and can be expanded in future studies, for example, to include softer soil conditions, or other tectonic settings.

Finally, this simulation model is ideal for performing scenario-based assessments because the input parameters, $F, M, R_{rup}$, and $V_{S30}$, define an earthquake design scenario. Intensity of shaking in the form of elastic response spectral ordinates is not a direct input parameter to the model. But, a post-processing procedure is suggested in the next section that extracts simulated ground motions for a specified shaking intensity from a pool of simulated motions for a specified design scenario.

## 3. STRUCTURAL ANALYSIS

The structures and analysis techniques used in this study are similar to those used in the Ground Motion Selection and Modification (GMSM) project (Haselton, 2009). The GMSM project was initiated to provide guidance and tools to the engineering community to facilitate selection of appropriate GMSM methods for nonlinear dynamic analyses. In this project, numerous existing ground motion selection and modification methods are evaluated and compared by determining their degrees of accuracy in predicting the structural response. To perform systematic studies, the GMSM project has carefully selected and designed several earthquake scenarios and a variety of nonlinear structures for analyses.

### 3.1. Structures

We select two structures from the GMSM project: buildings B and C. Both structures are modern reinforced concrete special moment frame buildings. They both consist of three-bay frames. The designs are code-conforming and were closely reviewed by a practicing engineer. Building B has 12 stories with a first-mode natural period of $T_{1,B} = 2.01$s. Building C is taller with 20 stories and a first-mode natural period of $T_{1,C} = 2.63$s. Additional information regarding the design of the selected structures and the modeling procedure can be found in Haselton (2009).

### 3.2. Earthquake and ground motion scenarios

For scenario-based assessments, we consider two earthquake scenarios that were developed in the GMSM project: M7 and M7.5. M7 Scenario is the occurrence of an earthquake on a strike-slip fault (i.e., $F = 0$) with a moment magnitude of 7.0 at a site that is 10km from the fault rupture on soil with $V_{S30} = 400$m/s. M7.5 Scenario is the same as the M7 Scenario, but with a moment magnitude of 7.5.

For intensity-based assessments, the ground motion for the M7 earthquake scenario is constrained to have a spectral acceleration at the building's first-mode, $S_a(T_1)$, that is two standard deviations above the median predicted value (i.e., $+2\epsilon$ motion). The ground motion for the M7.5 earthquake scenario is constrained to have a $S_a(T_1)$ value that is only one standard deviation above the median predicted value (i.e., $+1\epsilon$ motion). The constraints on the ground motions for each scenario were imposed by the GMSM project to ensure that the motions are consistent with typical 2% in 50 year motions and maximum considered earthquake (MCE) ground motions used in building code provisions. In this way, the database of simulated ground motions contains records that are capable of producing nonlinear behavior in the structures.

In this study, the M7 ground motion scenario ($F = 0$, $M = 7.0$, $R_{rup} = 10$km, $V_{S30} = 400$m/s, and $\epsilon = +2$) is applied to both buildings B and C. This helps us to study the differences between the two structures when they are subjected to a similar design scenario. The M7.5 ground motion scenario ($F = 0$, $M = 7.5$, $R_{rup} = 10$km, $V_{S30} = 400$m/s, and $\epsilon = +1$) is only applied to building C. This helps us to study the effects of the two design scenarios on building C responses.

### 3.3. Simulated ground motions for nonlinear dynamic analyses

Using the simulation method described in Section 2, we generated 750 records for the M7 design scenario (i.e., $F = 0$, $M = 7.0$, $R_{rup} = 10\text{km}$, $V_{S30} = 400\text{m/s}$) and 200 records for the M7.5 design scenario (i.e., $F = 0$, $M = 7.5$, $R_{rup} = 10\text{km}$, $V_{S30} = 400\text{m/s}$). More records were simulated for the first scenario because we wanted to have a decent number of simulations at the $+2\epsilon$ level. The second scenario requires fewer simulations because the desired shaking intensity is at only $+1\epsilon$. The 5% damped elastic response spectra of the two sets of simulated motions are shown in Fig. 3.1. In this figure, the statistics of the response spectral ordinates are also plotted. These statistics include the median, median ± 1 logarithmic standard deviation (i.e., $+1\epsilon$ motion), and median ± 2 logarithmic standard deviation (i.e., $+2\epsilon$ motion). The first-mode spectral periods of buildings B and C are also shown in each plot.

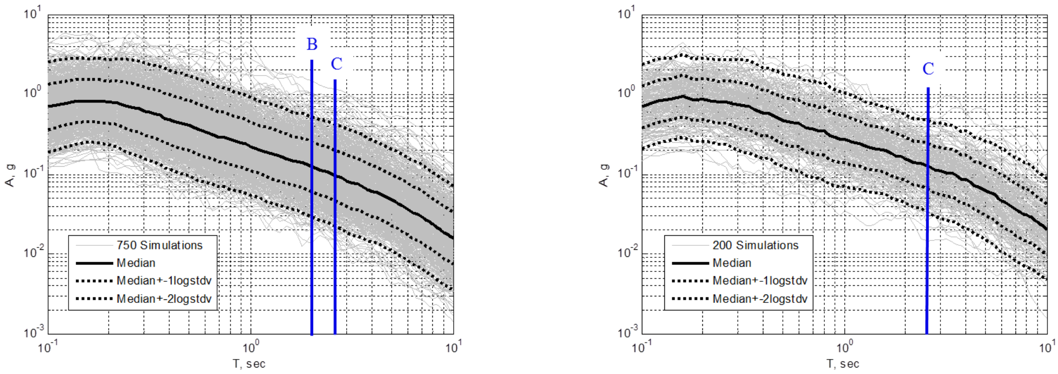


(a) (b)

**Figure 3.1.** Acceleration response spectra of (a) 750 simulated ground motions for the M7 earthquake scenario (b) 200 simulated ground motions for the M7.5 earthquake scenario.

Note that $R_{rup} = 10\text{km}$ is the minimum distance allowed, and $V_{S30} = 400\text{m/s}$ is outside the allowable range in the simulation model at its current state. We used the simulation method regardless of these restrictions because we wanted to perform our structural analyses for the same design scenarios used in the GMSM project, thereby allowing us to compare our resulting structural responses to those reported by the GMSM project. In future studies, the applicability range of the input variables to the simulation model can be modified to obtain more accurate simulations and structural responses.

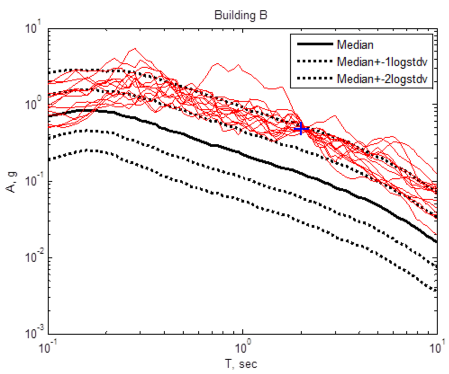


**Figure 3.2.** Selected motions for analyzing building B from the M7 Scenario simulations with specified shaking intensity of $+2\epsilon$.

The intensity of shaking in the form of response spectral values is not one of the input parameters to the simulation model. But it is a parameter specified in current building codes to efficiently estimate structural responses with few ground motions. To obtain records for the specified ground motion scenarios, we select simulations whose response spectral ordinates are within 10% of the target shaking intensity at the desired period. The target shaking intensity is calculated using the Campbell and Bozorgnia, 2008, GMPE. The spectral period is structure-dependent. Here, we only consider the first-mode period of the structure. Following this procedure, a total of 14 motions are selected from the M7 Scenario simulations at the $+2\epsilon$ shaking intensity for building B (Fig. 3.2). The $+$ sign in Fig. 3.2 indicates the target shaking intensity predicted by Campbell and Bozorgnia, 2008, GMPE. Similar figures are presented for the 18 selected simulations from the M7 Scenario (Fig. 3.3.a) and the 9 selected simulations from the M7.5 Scenario (Fig. 3.3.b) to analyze building C. Observe that the target shaking intensities for all three cases are in close agreement with the statistics of simulations (i.e., +1 and +2 standard deviations).

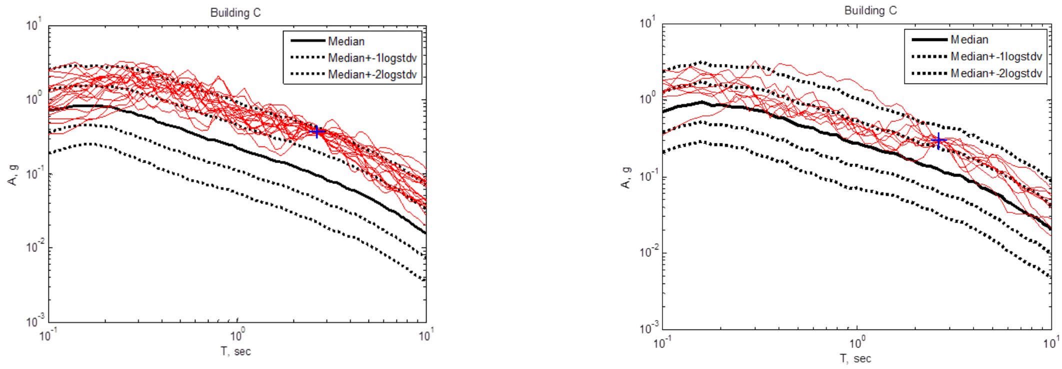


(a) (b)

**Figure 3.3.** Selected motions for analyzing building C from (a) the M7 Scenario simulations with specified shaking intensity of $+2\epsilon$, and (b) the M7.5 Scenario simulations with specified shaking intensity of $+1\epsilon$.

## 4. STRUCTURAL RESPONSES

The simulated ground motions in Section 3.3 are used as input excitations to buildings B and C to perform nonlinear dynamic analyses (see Haselton, 2009, for details of the structural analysis). Various structural responses were calculated, but in this paper, we focus on the maximum (over the building height) interstory drift ratio (MIDR). MIDR is also the response of interest in the GMSM project, where the "true" value of the median MIDR is calculated by using a large suite of earthquake records and performing extensive statistical analysis. This "true" value is referred to as the point of comparison (POC).

### 4.1. Intensity-based assessment

For intensity-based assessments, we need responses of the structures subjected to the ground motion simulations in Figs. 3.2 and 3.3. The results are summarized in Table 4.1 and plotted in Fig. 4.1. The median response is calculated and compared to the POC in the figure. Three ground motions collapse building B for the M7 scenario. The collapsed cases are not considered in the calculations of the mean response and the coefficient of variation (c.o.v). Compared to the scaling and modification methods investigated in the GMSM project, the agreement between our median response predictions and POCs is very good. The prediction bias factor, which is defined as the ratio between the median MIDR to the POC, is calculated for each case and is reported in Table 4.1.

**Table 4.1.** Statistics of the response (MIDR) for specified design scenarios and shaking intensities.

| | M7 Scenario, Building B (14 Records) | M7 Scenario, Building C (18 Records) | M7.5 Scenario, Building C (9 Records) |
|---|---|---|---|
| Median MIDR | 0.028 | 0.020 | 0.014 |
| Mean MIDR | 0.026 | 0.026 | 0.019 |
| c.o.v | 0.25 | 0.43 | 0.59 |
| Minimum MIDR | 0.014 | 0.020 | 0.009 |
| Maximum MIDR | 0.037 | 0.054 | 0.047 |

| | | | |
|---|---|---|---|
| POC | 0.022 | 0.019 | 0.016 |
| Prediction bias factor | 1.28 | 1.06 | 0.90 |

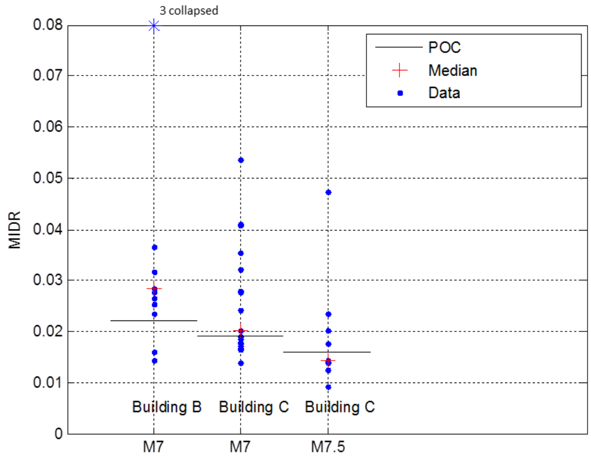


**Figure 4.1.** Structural responses (MIDR) to simulated ground motions at specified shaking intensities.

## 4.2. Scenario-based assessment

In intensity-based assessments, usually the median (or mean) response is of interest because few ground motions are considered and the small number of data is not adequate to predict the full-distribution of response. In addition to the median, the variability of response is an important factor. The next generations of seismic design procedures are moving towards a more performance-based analysis approach, where many intensity levels are considered and uncertainty of the response is quantified. For these types of scenario-based assessments, we calculate the structural response for all the ground motion simulations in Figure 3.1. This way, we can use the data to estimate the full-distribution of response. Fig. 4.2 shows the normalized frequency diagrams of MIDR. These plots can be used to estimate probability density functions (PDFs) of the response.

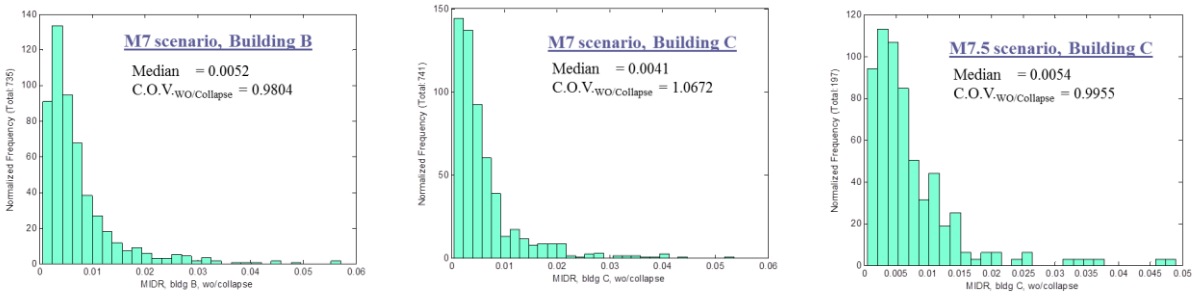


(a) (b) (c)

**Figure 4.2.** Normalized frequency diagrams of MIDR for the three cases under consideration.

### *4.2.1. Fragility curves and collapse probabilities*

One can generate empirical cumulative distribution functions (CDFs) for the response (i.e., integrals of the PDFs shown in Fig. 4.2 if the collapsed cases are also included). These functions are plotted in Fig. 4.3.a for the three cases under consideration and can be used to estimate the response fragility curves of buildings B and C for the specified design scenarios. These types of plots are extremely useful in probabilistic analyses and risk calculations because every level of response is associated with a level of probability. Additionally, Fig. 4.3.a can be used to study the differences between two structures (i.e., B and C) under the same design scenario. For example, the red and blue arrows in the figure indicate that there is a higher probability for MIDR of building C to be less than or equal to 0.01 if M7 earthquake scenario happens. We can also study the impacts of different earthquake scenarios on the same structure. For example, comparing the red and green arrows suggest that there is a greater probability of MIDR being less than or equal to 0.01 if the M7 Scenario occurs versus if the M7.5 scenario occurs.

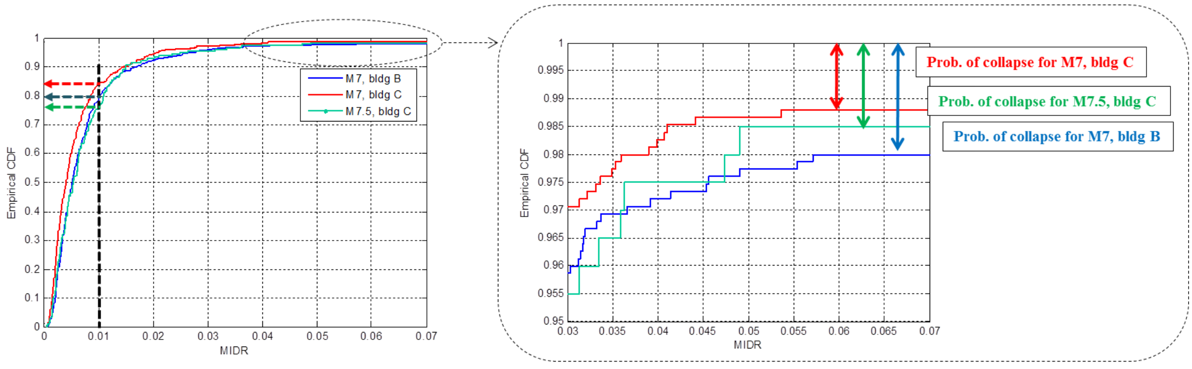


(a) (b)

**Figure 4.3.** Empirical cumulative distribution functions (CDFs) for MIDR for the three cases under consideration.

Fig. 4.3.b shows the empirical probability of collapse for each of the three cases under consideration. There is a greater probability of collapse for building C under the M7.5 Scenario compared to the M7 Scenario. Also, under the M7 earthquake scenario, building B has a greater chance to collapse than building C. This could be due to ground motions having a higher intensity level at the fundamental period of building B (see Fig. 3.1.a).

*4.2.2. Discussion: "full set" versus "selected set" of simulated motions*

If the objective of the analysis is to obtain the best estimate of the median (or mean) response using as few ground motion inputs as possible, an intensity-based assessment is ideal (see Fig. 4.4.a). In this case, a set of simulated ground motions are selected with intensities near the target shaking intensity. However, the resulting structural responses are not adequate enough to predict the full distribution or the variability of the response. If the full set of simulated ground motions for a specified design scenario are used, all possible intensities are considered and the resulting structural responses can be used to estimate the full distribution of the response for that specific design scenario. Fig. 4.4 demonstrates the difference between the predicted PDFs for these two cases for building B subjected to the M7 Scenario. Similarly, Fig. 4.5 illustrates this concept by using CDFs of the responses for buildings B and C under the M7 Scenario. Observe the smoothness of Figs. 4.4.b and 4.5.b compared to Figs. 4.4.a and 4.5.a.

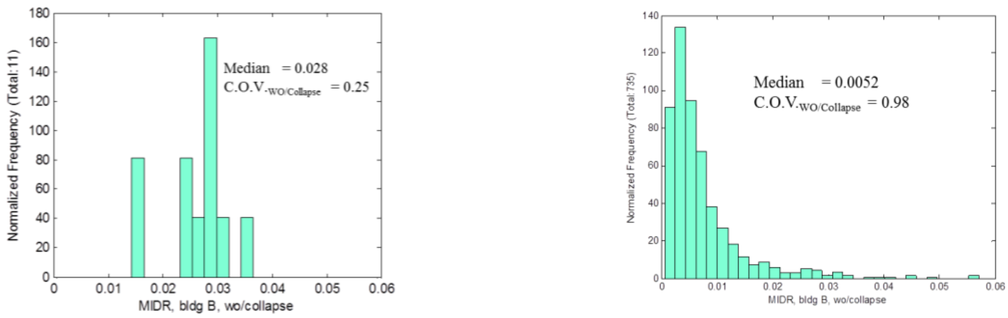


(a) (b)

**Figure 4.4.** Normalized frequency diagrams of MIDR for building B subjected to the M7 earthquake scenario for (a) a specified shaking intensity of $+2\epsilon$, and (b) all possible shaking intensities.

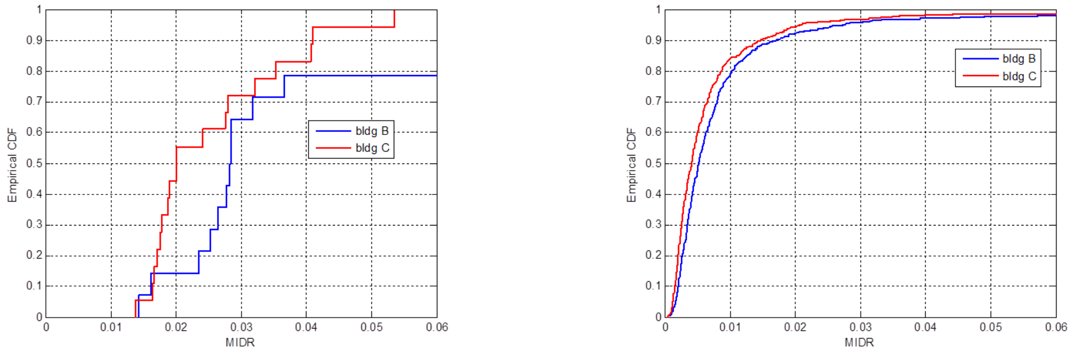


(a) (b)

**Figure 4.5.** Empirical CDFs of MIDR for buildings B and C subjected to the M7 earthquake scenario for (a) a specified shaking intensity of $+2\epsilon$, and (b) all possible shaking intensities.

## 4.3. Time-based assessment

Advancing from an intensity-based to a scenario-based assessment requires consideration of all possible intensity levels for a specified design scenario (i.e., specified $F, M, R_{rup}$, and $V_{S30}$). For time-based assessment, we need to move one step further and consider all the possible design scenarios in a specified period of time. Therefore, ground motions should be simulated for various design scenarios (i.e., multiple sets of simulations similar to Fig. 3.1 are required). Combining the resulting structural responses with the frequency of each design scenario allows one to perform risk calculations and to determine the probability of collapse in the specified period of time.

## 5. CONCLUSIONS

A stochastic simulation method is used to generate earthquake ground motions for two design scenarios defined by their faulting mechanism, earthquake magnitude, source-to-site distance, and soil conditions. These simulations are used to perform intensity-based and scenario-based assessments of two structures. The structural response, MIDR, and its statistics are examined and compared to the results of the GMSM project. Finally, the extension to perform time-based assessments is discussed.


## AKCNOWLEDGEMENT

The structural analyses reported in this study were performed by Dr. Curt Haselton. His efforts and collaboration during the course of this study are greatly appreciated.


## REFERENCES


(ATC-58-1) Applied Technology Council (2011). *Seismic Performance Assessment of Buildings, Volume 1-Methodology*, 75% draft, Redwood City, CA.

Campbell, K.W. and Bozorgnia, Y. (2008). NGA ground motion model for the geometric mean horizontal component of PGA, PGV, PGD and 5% damped linear elastic response spectra for periods ranging from 0.01 to 10s. *Earthquake Spectra*, **24**, 139-171.

Dabaghi, M., Rezaeian, S. and Der Kiureghian, A. (2011). Stochastic simulation of near-fault ground motions for specified earthquake and site characteristics. *Proceedings of the International Conference on Appliations fo Statistics and Probability in Civil Engineering (ICASP)*, Zurich, Switzerland.

Haselton, C.B. (2009). *Evaluation of Ground Motion Selection and Modification Methods: Predicting Median Interstory Drift Response of Buildings*, Pacific Earthquake Engineering Research Center, Berkeley, CA.

Rezaeian, S. and Der Kiureghian, A. (2010). Simulation of synthetic ground motions for specified earthquake and site characteristics. *Earthquake Engineering and Structural Dynamics*. **39**, 1155-1180.

Rezaeian, S. and Der Kiureghian, A. (2012). Simulation of orthogonal horizontal ground motion components for specified earthquake and site characteristics. *Earthquake Engineering and Structural Dynamics*. **41**, 335-353.